

Measurement of bioelectric and acoustic profile of breast tissue using hybrid magnetoacoustic method for cancer detection

M. I. Mohamad Salim · E. Supriyanto ·
J. Haueisen · I. Ariffin · A. H. Ahmad ·
B. Rosidi

Received: 5 August 2012 / Accepted: 3 December 2012 / Published online: 14 December 2012
© International Federation for Medical and Biological Engineering 2012

Abstract This paper proposes a novel hybrid magnetoacoustic measurement (HMM) system aiming at breast cancer detection. HMM combines ultrasound and magnetism for the simultaneous assessment of bioelectric and acoustic profiles of breast tissue. HMM is demonstrated on breast tissue samples, which are exposed to 9.8 MHz ultrasound wave with the presence of a 0.25 Tesla static magnetic field. The interaction between the ultrasound wave and the magnetic field in the breast tissue results in Lorentz Force that produces a magnetoacoustic voltage output, proportional to breast tissue conductivity. Simultaneously, the ultrasound wave is sensed back by the ultrasound receiver for tissue acoustic evaluation. Experiments are performed on gel phantoms and real breast tissue samples harvested from laboratory mice. Ultrasound wave characterization results show that normal breast tissue experiences higher attenuation compared with cancerous tissue. The mean magnetoacoustic voltage results for normal tissue are lower than that for the cancerous tissue

group. In conclusion, the combination of acoustic and bioelectric measurements is a promising approach for breast cancer diagnosis.

Keywords Breast cancer · Magnetism · Ultrasound · Tissue conductivity · Tissue density

1 Introduction

Breast cancer is the most common cancer in women worldwide which accounts for approximately 25 % of all female malignancies [8]. Breast cancer is characterized by uncontrolled breast cells growth, in which the cells acquire genetic alteration that allows them to proliferate outside the context of normal tissue development [20]. In the cancerous tissue, changes in density occur due to uncontrolled cell multiplication [20], excessive accumulation of protein in stroma [1] and enhancement of capillary density from the preexisting vascular network or also known as angiogenesis [28]. On the other hand, changes in conductivity also occur due to the increase of cellular water and electrolyte content as well as altered membrane permeability and blood perfusion to support high metabolism requirements of a malignant cell [5, 20]. There is also enough evidence from literature indicating that, compared with normal tissue, malignant tissue has higher conductivity [6, 30] and permittivity [14, 27] but lower in impedivity [2, 13]. Given these changes, a hybrid measurement technique seems very suitable to assess the acoustic and bioelectric properties of normal and cancerous breast tissues. An acoustic evaluation of tissue is very useful in estimating tissue density as the ultrasound attenuation level in tissue changes with density [16]. A bioelectric evaluation reveals information related to tissue conductivity. This hybrid

M. I. M. Salim (✉) · E. Supriyanto
Department of Clinical Sciences, Faculty of Biosciences
and Medical Engineering, Universiti Teknologi Malaysia,
81310 Johor Bahru, Malaysia
e-mail: maheza@biomedical.utm.my

J. Haueisen
Institute of Biomedical Engineering and Informatics,
Ilmenau University of Technology, Ilmenau, Germany

I. Ariffin · A. H. Ahmad
Department of Electronics, Faculty of Electrical Engineering,
Universiti Teknologi Malaysia, 81310 Johor Bahru, Malaysia

B. Rosidi
Mochtar Riady Institute for Nanotechnology, Jalan Boulevard
Jend. Sudirman 1688, Lippo Karawaci, Tangerang,
Banten 15810, Indonesia

system is inspired from the previous magnetoacoustic techniques used to assess bioelectric property only.

Historically, the research in magnetoacoustic measurement system has begun since 1988 by the work of Towe and Islam in the development of one-dimensional, noninvasive magnetoacoustic system [31]. This system applies a simultaneous combination of time-varying magnetic field and static magnetic field onto a conductive object under test. Time varying magnetic field induces an eddy current in the object volume. The eddy current in a static magnetic field produces vibration due to Lorentz force and emits sound wave in the frequency of the stimulated alternating magnetic field with intensity that is proportional to the object conductivity [17]. Hence, the term magnetoacoustic represents a combination of magnetic field as the input and acoustic as the output. This very first system was tested to measure bioelectric current in a living hamster. The resulting vibration was easily detected using microphone since the frequency of the stimulating magnetic field was in the range of audible frequency. In 1994, a complete theoretical model of magnetoacoustic technique for bioelectric current was published by Roth et al. [26]. The theoretical model is based on the fundamental equation of continuum mechanics and electromagnetism where feasibility measurement of bioelectric current in vitro and in vivo is discussed. Later in 2006, Bin He et al. improved the first system with the development of Magneto Acoustic Tomography with Magnetic Induction (MATMI) [17]. In MATMI, time varying magnetic field at the range of ultrasonic frequency is used to produce image mapping with a resolution close to sonography [17]. MATMI was tested to image a wire phantom as well as real biological tissue with different conductivity in vitro. The result showed that MATMI was capable to produce a high-resolution image and was sensitive to differentiating various types of tissue with different conductivity in the image.

In 1998 Wen et al. [35] developed another approach of magnetoacoustic system by combining static magnetic field and sound wave onto a conductive medium. Propagation of ultrasound induces the motions of ion in the medium. Moving ions in a static magnetic field are subjected to Lorentz force effect that separates the charges according to their polarity. This charge separation creates detectable electrical potential or voltage that is proportional to the conductivity of the medium [34]. Hence, in this approach, magnetoacoustic refers to the combination of magnetic field and acoustic as inputs. The system was tested to image a polycarbonate phantom and biological tissue [33]. A further study by Su et al. [29] had improved Wen's technique when a focused ultrasound transducer was used to focus the sound wave at a focal point to maximize the interaction effects and increase the resulting voltage value

at that point. As a result, a better voltage value was obtained for the conductivity profile assessment of tissue.

Previous magnetoacoustic methods manipulated magnetoacoustic interaction for bioelectric profile assessment only. The output of stimulated ultrasound that was used to initiate electrical charge movement in the second approach was ignored, although it presumably contained valuable information with regards to tissue density. In addition to that, the magnetoacoustic techniques were so far not applied to study pathological tissue, such as cancerous tissue. Hence, this study proposes the concept of hybrid magnetoacoustic measurements (HMM) which considers the acoustic and bioelectric outputs for breast cancer detection.

2 Materials and methods

Theoretically, the HMM system that is developed in this study manipulates the interaction between the ultrasound wave motion and magnetic field onto ions or electrical charges in a conductive media such as breast tissue based on the second approach of magnetoacoustic technique. Consider an ion in a breast tissue sample with charge q that is exposed to ultrasound wave from z direction and magnetic field from y direction. The longitudinal motion of an ultrasound wave in z direction will cause the ion to oscillate back and forth in the medium with velocity \mathbf{V}_0 . In the presence of constant magnetic field \mathbf{B}_0 in y direction, the ion is subjected to the Lorentz Force [35].

$$\mathbf{F} = q[\mathbf{v}_z \times \mathbf{B}_0] \quad (2.1)$$

From (2.1), the equivalent electric field is [23]

$$\mathbf{E}_0 = \mathbf{v}_z \times \mathbf{B}_0 \quad (2.2)$$

The field \mathbf{E}_0 and current density \mathbf{J}_0 oscillate at the ultrasonic frequency in a direction mutually perpendicular to the ultrasound propagation path and the magnetic field \mathbf{B}_0 (x direction). The electric current density is given by [23, 35]

$$\mathbf{J}_0 = \sigma[\mathbf{v}_z \times \mathbf{B}_0] \quad (2.3)$$

Finally, the magnetoacoustic voltage, \mathbf{V} across a set of measurement electrodes a and b due to \mathbf{J}_0 can be calculated following the reciprocity theorem defined elsewhere [29]:

$$\mathbf{V} = \iiint [(\mathbf{v}_z \times \mathbf{B})\mathbf{J}_{ab}/\mathbf{I}]dV \quad (2.4)$$

where \mathbf{J}_{ab} is the current density that is induced under the electrode surface in the breast tissue if an one-ampere current, \mathbf{I} , is applied onto the sample through the measurement electrodes [29]. The measured voltage is proportional to the tissue conductivity and velocity of ions induced by the ultrasound motion in the tissue.

Simultaneously, the ultrasound wave input that is initially used to induce ionic motion inside the tissue will be sensed back for tissue acoustic evaluation.

2.1 Experimental setup

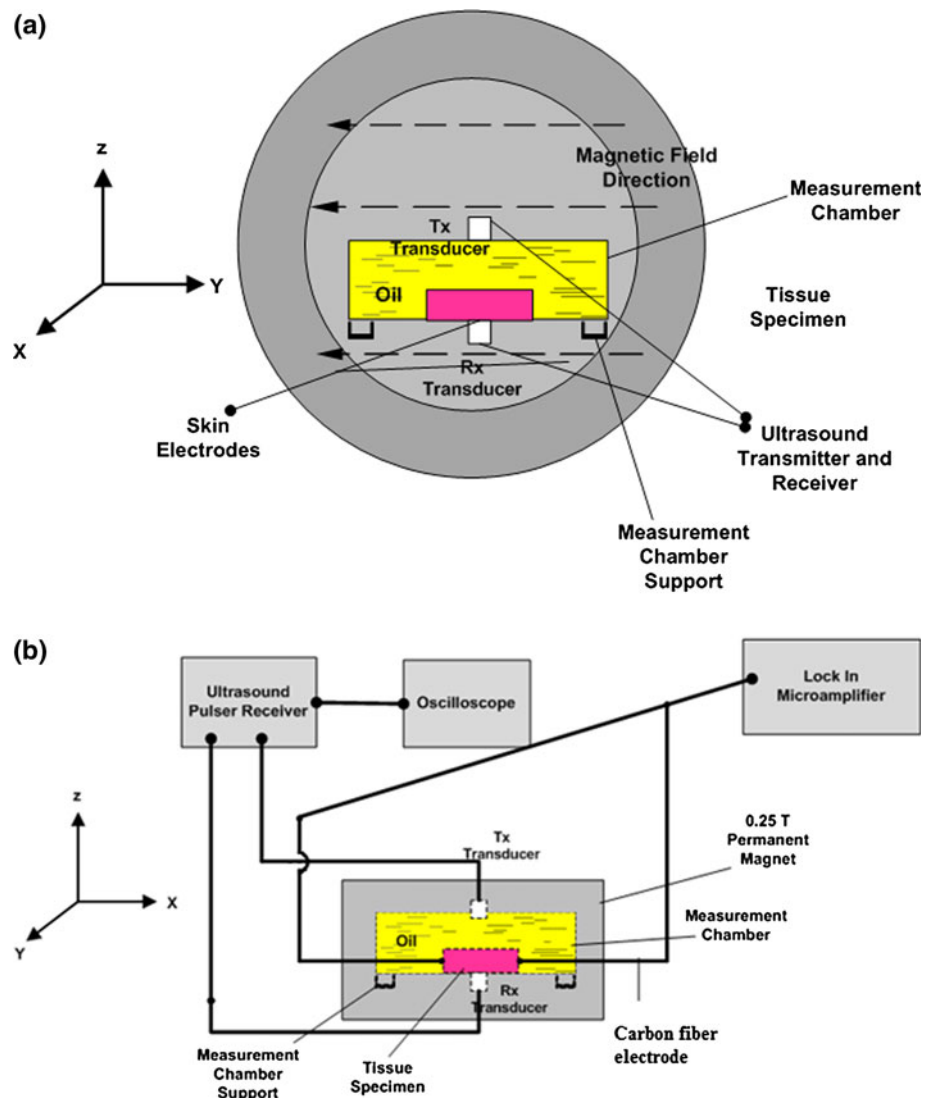
This experimental study was conducted in an anechoic chamber with shielding from 18 kHz to 40 GHz. The HMM system consists of a 5077PR Manually Controlled Ultrasound Pulser Receiver unit (Olympus-NDT, Massachusetts, USA). The unit was set to deliver 400 V of negative square wave pulses at the frequency of 10 MHz and PRF of 5 kHz, to 2 units of 0.125 inch standard contact, single element ceramic ultrasound transducers having peak frequency at 9.8 MHz. Transducers were used to transmit and receive the ultrasound wave in the transmission mode setting from the z direction. The pulser receiver unit was also attached to a digital oscilloscope (model TDS 3014B, Tektronix, OR, USA) for signal display and storage purposes.

A custom-made, 15 cm height, diameter pair magnetized NdFeB permanent magnet was used to produce static magnetic field, with the intensity of 0.25 T at the center of its bore with homogeneity of 45 ppm. The diameter of the magnet bore was 5 cm and the direction of magnetic field was set from y axis (see Fig. 1), whilst the real experimental assembly is shown in Fig. 2.

Magnetoacoustic voltage measurements were conducted from the x direction with respect to measurement chamber by using 2 units ultrasensitive carbon fiber electrodes (ALA Scientific Inc, Farmingdale, USA). Carbon fiber electrodes provide low noise measurements [7] and have very weak paramagnetic properties compared with conventional electrodes [3, 19]. In addition to that, studies reported that carbon fiber electrodes have sensitivity down to 1 nV [21].

In this study, the carbon fiber electrodes were connected to a high-frequency lock-in amplifier (model SR844, Stanford Research System, CA, USA). The full-scale sensitivity of the amplifier is 100 nV_{rms}. Magnetoacoustic

Fig. 1 Block diagram of the hybrid magnetoacoustic system **a** side view. **b** Cross-sectional view (not to scale)



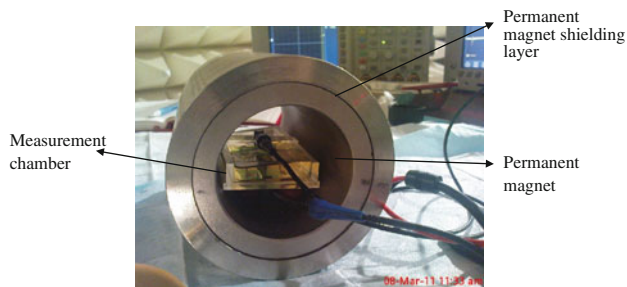


Fig. 2 Real experimental assembly that consists of a measurement chamber which placed the tissue sample inside the permanent magnet bore. It was filled by non-conducting oil to prevent ultrasound leakage current from contaminating the magnetoacoustic voltage measurements. Ultrasound transmitter and receiver are attached to the measurement chamber from the z direction

voltage measurement was made by touching the electrodes onto the tissue in x direction. Figure 1 shows the block diagram of Hybrid Magnetoacoustic System.

2.2 Preparation of samples

Two types of samples were used in this study. The first sample was a set of tissue-mimicking gel that was designed with properties of normal breast tissue. Another sample was a set of animal breast tissues that was harvested from a group of tumor-bearing laboratory mice and its control strain. The tissue mimicking gel was used in the early part of this study to understand the basic response of HMM system to linear samples before it was tested to complex samples like real tissues.

The use of animal in this study was approved by the National University of Malaysia Animal Ethics Committee. Transgenic mice strains FVB/N-Tg MMTV PyVT 634 Mul and its control strain FVB/N were obtained from the Jackson Laboratory, USA. Transgene expression of the mice strain is characterized by the development of breast cancer which usually metastasizes to lung cancer in both male and female carriers with 100 % penetrance at 40 days of age [32]. All female carriers are capable to develop palpable cancer from as early as 5 weeks of age [10]. The breast cancer that arose was observed to be multifocal, highly fibrotic and involved the entire mammary fat pad [10]. Mice carrying the PyVT transgene also showed loss of lactational ability since the first pregnancy [32].

The female mice were palpated every 3 days from 12 weeks of age to identify tumors. They were used as subjects when their tumor diameter reached 2 cm or when they reached 18 weeks of age for normal mice. During the surgery procedure, anesthesia was performed using the Ketamin-Xylazil-Zoletil cocktail dilution. 0.2 ml of the anesthetic drug was administered intravenously from the mouse tail and an additional of 2 ml of the drug was delivered intraperitoneally. Fur around the breast area was shaven. Excised breast specimens were cut down to an

Table 1 Weight variation of tissue specimen

No.	Tissue group	Weight variation mean \pm SD (g)
1	Cancerous tissue	0.257 ± 0.03
2	Normal tissue	0.225 ± 0.02

approximately 1 cm \times 1 cm square shape with thickness of 2 mm immediately after the surgery to maintain the tissue physiological activities. Each tissue was carefully trimmed down to the required thickness and the standardization was made using a custom-made U -shaped mold with 2 mm opening. The mice were then euthanized by using drug overdose method.

The overall process of trimming down after excision took an average time of 6 min and the samples were immediately immersed in the measurement chamber for scanning to maintain their physiological activities [6, 30]. A total of 24 normal and 25 cancerous breast tissue specimens were used in this study and the variation in the tissue weight for normal and cancerous tissue group is presented in Table 1.

2.3 Measurement and analysis

Three different types of measurements were conducted in this study: conductivity and density measurements, HMM ultrasound measurements and HMM magnetoacoustic voltage measurements.

In conductivity and density measurements, one sample of gel, one sample of real tissue from the normal and the cancerous group were selected for conductivity and density measurements. Density measurement involves the quantification of tissue mass and volume of each sample. The final sample density was calculated by dividing the average tissue mass with its average tissue volume. On the other hand, the conductivity measurement was performed using the potential divider method. The potential divider method is a simplification of Wheatstone bridge method as used by Fricke et al. to determine unknown electrical conductivity or resistance of tissue including fat, gland, mastitis, fibroadenoma and carcinoma by measuring its parallel capacitance and resistance [27].

In HMM ultrasound measurement, all samples were immersed in measurement chamber and their positions were aligned with the position of ultrasound transmitter and receiver [22]. Then their positions were fixed using a nylon fiber. The ultrasound transmitter emitted 9.8 MHz ultrasound wave in a transmission mode from the z direction. The distance between the ultrasound transmitter and receiver was set constant to 6 mm. Measurement was performed using the insertion loss method [9, 36] at a constant temperature of 21 °C. Vegetable oil was used as medium for ultrasound propagation to prevent any leakage

of current from contaminating the measurement chamber and interfering with the HMM magnetoacoustic voltage output [29]. Measurement was repeated for 5 times for every biological sample at any random position on the sample surface and 2 times for gel samples.

Simultaneously, the magnetoacoustic voltage measurement was made by touching the carbon fiber electrodes onto the tissue surface from the *x* direction. The electrodes were attached to the SR844 lock-in amplifier for signal detection and recording. The resulting magnetoacoustic voltage was in the form of digital reading displayed by the lock-in amplifier indicating the value of the acoustically induced magnetoacoustic voltage in the samples along the duration of ultrasound propagation.

The electrode tip was the only contact point between the tissue and the detection circuit. The input impedance of the lock-in amplifier was set to 1 MΩ while the time constant was set to 3 ms. The experimental reading was updated every 1 s since the amplifier requires a few times of constant cycle to stabilize the output reading. In this study, the lock-in amplifier functions as a high-precision voltage reader and a filter that detects signal as low as 100 nV at 9.8 MHz and eliminates other surrounding noises. Measurement was repeated ten times for every biological tissue sample and two times for gel samples.

The ultrasound data were further processed to calculate the power spectral density of the signal in Matlab (The MathWorks, Natick MA, USA). The processing steps involved the determination of frequency content of an ultrasound waveform via frequency decomposition to find its attenuation in each tissue group and gel. The attenuation level was calculated by subtracting the log mean squared spectrum of the ultrasound signal propagating through the oil without tissue (P_0), by the log mean squared spectrum of ultrasound signal propagating through the oil with tissue (P_s), following the equation [9, 36]:

$$\text{Attenuation (dB)} = 10 (\log P_0 - \log P_s) \tag{3.14}$$

Later, all HMM ultrasound attenuation and HMM magnetoacoustic voltage data were statistically analyzed

Table 2 Conductivity and density value for each tissue group measured from one random sample

Samples	Conductivity S/m	Density (kg/m ³)
Normal mice breast	0.239	1,121
Cancerous mice breast	0.547	1,319
Gel	0.270	1,114

in PASW statistics 18 software (SPSS Ltd, Quarry Bay, Hong Kong). Paired sample *t* test was used to test the significance of numerical mean differences between the normal and cancerous group.

3 Results

3.1 Conductivity and density measurements

The conductivity and density measurement results shown in Table 2 indicate that cancerous mice breast tissue has higher density and conductivity compared with its corresponding normal tissue. This finding agrees well with the expectations. In addition to that, the conductivity and density measurement results for gel are close to that of the normal tissue as it is designed to resemble the characteristics of a normal tissue.

3.2 Ultrasound measurements

Table 3 shows the statistical analysis result including mean and standard deviation of tissue acoustic attenuation and magnetoacoustic voltage from samples in this study.

The HMM ultrasound measurement result shows that normal breast tissue attenuates ultrasound energy at a higher rate compared with the cancerous tissue group whilst the gel phantom attenuates the ultrasound energy even less. The obtained result also shows that a small part of the attenuation level of normal and cancerous tissue overlapped due to its large standard deviation. However, paired *t* test result shows a significant difference in

Table 3 Overall HMM output

Type of sample	Number of ultrasound measurements	Number of voltage measurements	Attenuation scale (dB mm ⁻¹) mean ± SD	Magnetoacoustic voltage (μV) mean ± SD
Tissue mimicking gel	30	30	0.501 ± 0.440	0.56 ± 0.21
Normal breast tissue	106	212	2.329 ± 1.103	0.42 ± 0.16
Cancerous breast tissue	106	212	1.760 ± 1.080	0.80 ± 0.21

ultrasound attenuation between normal and cancerous tissue group ($p < 0.0001$).

3.3 Magnetoacoustic voltages

The magnetoacoustic voltage measurement result shows that its value is the highest for the cancerous tissue group, followed by the gel group and finally the normal tissue group (Table 3). Paired t test result also shows a significant difference in magnetoacoustic voltage value between the normal and cancerous group ($p < 0.0001$).

The voltage value for cancerous tissue is high since it has a high conductivity value. However, the measured magnetoacoustic voltage values for gel and normal tissue are different though the conductivities of normal tissue and homogenous gel are almost the same. In general, it is noted from the ultrasound measurement result that normal tissue group highly attenuates ultrasound energy. In the case of large amount of attenuation, the sound energy that is left to move the particles in the tissue decreases. Hence, the resulting particle velocity is reduced and consequently, the value of the acoustically induced magnetoacoustic voltage is also lower for the normal tissue.

4 Discussion

Absorption, scattering and reflection are the processes that contribute to ultrasound energy attenuation in tissue, with absorption being considered as the most dominant factor [4, 11]. Tissue mimicking gel that is used in this study has a homogenous structure. The attenuation level is very small and is mainly contributed by the absorption process (scattering and reflection inside the gel are minor). The observed standard deviation of the attenuation is also smaller compared with real biological tissue due to the structural homogeneity. On the contrary, a real breast tissue has a complex and heterogeneous structure. It consists of viscous extracellular matrix and individual cells with elastic membrane and viscous cytoplasm [12, 15, 18]. As ultrasound wave travels through a viscoelastic media, the molecules in the medium move back and forth from their equilibrium position. This movement requires energy that is provided to the medium by the ultrasound source, causing ultrasound energy dissipation via absorption process. Normal breast tissue is considered to be more viscoelastic than a cancerous tissue. Hence, the molecules in normal tissue have more freedom of motion and are capable to have larger displacement and longer oscillation when induced with ultrasound, compared with the elastic and high-density cancerous tissue [25]. Its dense property gives the cancerous tissue higher inertia to resist displacement and acceleration that are caused by the

ultrasound wave at its resting state [24]. Therefore, the energy of ultrasound beam is reduced in a higher rate as it passes the viscoelastic normal tissue compared with a more elastic cancerous tissue [24]. Another factor of attenuation is the reflection process that occurs at the interface between the oil and the tissue. The amount of reflection at the interface is determined by the acoustic impedance difference between the oil and its adjacent medium. In addition to that, the heterogeneity of the breast tissue encourages further energy loss due to scattering [24]. This complex cellular and tissue heterogeneity is likely the cause for the relatively high standard deviation of the attenuation levels for both tissue groups.

The measured magnetoacoustic voltages in Table 3 are found to be in principle agreement with the theoretically predicted magnetoacoustic voltage based on the simplified model calculations outlined in Sect. 1.2 (last row in Table 4). Table 4 also gives a comparison of the parameters of HMM and the Magneto-Acousto electrical Tomography (MAET) [29]. MAET uses the same magnetoacoustic approach as HMM and shares the same fundamental calculation principle in estimating the voltage output. Hence, MAET is the closest approach to HMM.

The estimated calculation of MAET [37] is conducted using static magnetic field with field intensity of 1T. In HMM, fourfold lower magnetic field intensity is used and the result is proportional to MAET. In general, the application of higher magnetic field intensity requires higher production cost for better permanent magnet materials and design. On the other hand, lower field intensity magnet is cheaper but a proper voltage detection circuit is necessary since the signal level is within the range of ambient noise. Unlike HMM, the final amplitude of MAET signal is higher and is less vulnerable to ambient noise due to the stronger magnetic field.

HMM uses higher ultrasound wave frequency compared with MAET. High-frequency ultrasound offers high-

Table 4 Comparison of parameters for HMM and MAET

Parameter	HMM	MAET [37]
Material	Biological tissue (0.2–0.5 S/m)	Agar gel (0.5 S/m)
Magnetic induction	0.25 T	1 T
Ultrasound frequency (MHz)	9.8	2.25
Specimen volume	$3.88e^{-10} \text{ m}^3$	$2e^{-9} \text{ m}^3$
Distance of ultrasound propagation path in z direction (mm)	6	100
Distance between 2 electrodes (mm)	10	50
Calculated magnetoacoustic voltage	$5.43e^{-6} \text{ V}$	$21.39e^{-6} \text{ V}$

resolution information when the sound wave propagates through tissues. However, the attenuation of higher frequency ultrasound is also high, limiting its propagation distance to only thinner materials.

Overall, the amplitude of the final magnetoacoustic voltage signal generated by MAET is fourfold higher than the calculated value of HMM output. This observation complies very well with the previous study by Wen et al. [29, 33, 34] that stated the amplitude of magnetoacoustic voltage signal is linearly proportional to the particle velocity induced by the ultrasound propagation and also magnetic field intensity. Since the particle velocity induced by ultrasound ranges only 1,400–1,600 m s⁻¹ in soft tissues, the resulting fourfold increase in MAET voltage amplitude is proportional to its higher magnetic field intensity.

In conclusion, this work has proposed a new Hybrid Magnetoacoustic approach which is capable of accessing simultaneously the electric and acoustic properties of tissue. The experimental results show that HMM can be a promising tool for breast cancer detection. HMM has low costs and can be easily incorporated into the existing MRI setups. Further research will concentrate on the development of a 2D HMM system for breast imaging.

Acknowledgments The authors would like to acknowledge Ministry of Higher Education of Malaysia for the award of Fundamental Research Grant Scheme Vote 78371 entitled “A Novel Tissue Imaging Method using short pulse magnetoacoustic wave” and Universiti Teknologi Malaysia for the Institutional Research Grants Vote 77535 and 77202.

References

- Arendt ML, Rudnick JA, Keller PJ, Kuperwasser C (2010) Stroma in breast development and disease. *Semin Cell Dev Biol* 21:11–18
- Association for the Advancement of Medical Instrumentation (1993) American National Standard: Safe Current Limit for Electromedical Apparatus. Arlington, Document ANSI/AAMI ES1-1993
- Austin VC, Blamire AM, Grieve SM, O'Neill MJ, Styles P, Matthews PM, Sibson NR (2003) Differences in the BOLD fMRI response to direct and indirect cortical stimulation in the rat. *Magn Reson Med* 49:838–847
- Berger G, Laugier P, Thalabard JC, Perrin J (1990) Global breast attenuation: control group and benign breast diseases. *Ultrason Imaging* 12:47–57
- Blad B, Baldertorp B (1996) Impedance spectra of tumor tissue in comparison of normal tissue: a possible clinical application for electrical impedance tomography. *Physiol Meas* 17:105–115
- Chaudary SS, Mishra RK, Swarup A, Thomas JM (1984) Dielectric properties of normal and malignant human breast tissue at microwave and radiowave frequencies. *Indian J Biochem Biophys* 21:76–79
- Crespi F, England T, Ratti E, Trist DG (1995) Carbon fibre micro-electrodes for concomitant in vivo electrophysiological and voltammetric measurements: no reciprocal influences. *Neurosci Lett* 188:33–36
- Cuzick J (2003) Epidemiology of breast cancer—selected highlights. *Breast* 12:405–411
- Edmonds PD, Mortensen CL (1991) Ultrasonic tissue characterization for breast biopsy specimen. *Ultrason Imaging* 13(2):162–185
- Guy CT, Cardiff RD, Muller WJ (1992) Induction of mammary tumors by expression of polyomavirus middle T oncogene: a transgenic mouse model for metastatic disease. *Mol Cell Biol* 12(3):954–961
- Johnson SA, Abbott T, Bell R, Berggren M, Borup D, Robinson D, Wiskin J, Olsen S, Hanover B (2007) Non-invasive breast tissue characterization using ultrasound speed and attenuation -in vivo validation. *Acoust Imaging* 28:147–154
- Johnson-Selfridge P, Selfridge RA (1985) Approximate materials properties in isotropic materials. *IEEE Trans. Ultrasonic Ferroelectric Freq Control* SU-32, p 381
- Jossinet J (1996) Variability of impedivity in normal and pathological breast tissue. *Med Biol Eng Comput* 34:346–350
- Jossinet J, Lobel A, Michoudet C, Schmitt M (1985) Quantitative technique for bio-electrical spectroscopy. *J Biomed Eng* 7:289–294
- Kelley JF, McGough RJ (2009) Fractal ladder models and power law wave equation. *J Acoust Soc Am* 126(4):2072–2081
- Landini L, Sarnelli S (1986) Evaluation of the attenuation coefficient in normal and pathological breast tissue. *Med Biol Eng Compu* 24:243–247
- Li X, Xu Y, He B (2006) A phantom study of magnetoacoustic tomography with magnetic induction (MAT-MI) for imaging electrical impedance of biological tissue. *J Appl Phys* 99(6):066112
- Lim CT, Zhou EH, Quek ST (2000) Mechanical model for living cell: a review. *J Biomech* 39:195–216
- Lin J, Sun S, Chen C, Chang W, Hou B, Shyu BC (2004) A fMRI study of the anterior cingulate cortex activations during direct electrical stimulation of the medial thalamus in rats. *J Neurosci Method* 137:123–131
- Locasale JW, Cantley LC (2010) Altered metabolism in cancer. *BMC Biol* 88:88
- Miller PR, Gittard SD, Edward TL, Lopez DM, Xiao X (2011) Integrated carbon fiber electrodes within hollow polymer micro-needles for transdermal electrochemical sensing. *Biomicrofluidics* 5-013415:1–14
- Mohamad Salim MI, Ahmmad SNZ, Rosidi B, Ariffin I, Ahmad AH, Supriyanto E (2010) Measurements of ultrasound attenuation for normal and pathological mice breast tissue using 10 MHz ultrasound wave. In: *Proceeding of the 3rd WSEAS international conference on visualization, imaging and simulation (VIS'10)*, November 3–5, 2010. WSEAS; Faro, Portugal, pp 118–122
- Norton SJ (2003) Can ultrasound be used to stimulate nerve tissue? *Biomed Eng Online* 2:1–9
- Norton M, Karczub D (2003) *Fundamentals of noise and vibration analysis for engineer*, 2nd edn. Cambridge Press, Cambridge
- Provenzano PP, Inman DR, Eliceiri KW, Knittel JG, Yan L, Rueden CT, White JG, Keely PJ (2008) Collagen density promotes mammary tumor initiation and progression. *BMC Med* 6(11):1–15
- Roth BJ, Basser PJ, Wiksowo JP (1994) A theoretical model for magneto-acoustic imaging of bioelectric currents. *IEEE Trans Biomed Eng* 41(8):723–728
- Sha L, Ward ER, Story B (2002) A review of dielectric properties of normal and malignant breast tissue. In: *Proceeding of IEEE SoutheastCon 2002*, IEEE, pp 457–462
- Shinoji M, Hancock WW, Abe K, Micko C, Casper KA, Baine RM (1998) Activation of coagulation and angiogenesis in cancer:

- immunohistochemical localization in situ of clotting proteins and vascular endothelial growth factor in human cancer. *Am J Pathol* 152(2):399–411
29. Su Y, Haider S, Hrbek A (2007) Magnetoacousto electrical tomography, a new imaging modality for electrical impedance. In: 13th international conference on electrical bioimpedance and the 8th conference on electrical impedance tomography IFMBE proceeding, August 29–Sept, 2007. Springer, Graz, pp 292–295
 30. Surowiec AJ, Stuchly SS, Barr JB, Swarup A (1988) Dielectric properties of breast carcinoma and the surrounding tissue. *IEEE Trans Biomed Eng* 35:257–263
 31. Towe BC, Islam MR (1988) A magneto acoustic method for the noninvasive measurement of bioelectric current. *IEEE Trans Biomed Eng* 35(10):892–894
 32. The Jackson Laboratory (2010) JAX Mice Database: MMTV-PyVT strain, USA
 33. Wen H, Bennet E (2000) The feasibility of Hall effect imaging in humans. 2000 IEEE Ultrasonic Symposium, October 22–25, IEEE; San Juan, Puerto Rico, pp 1619–1622
 34. Wen H, Bennett E, Shah J, Balaban RS (1997) An imaging method using ultrasound and Magnetic Field. In: Proceeding of the 1997 IEEE ultrasonic symposium. October 5–8, 1997. IEEE; Toronto, Ontario, pp 1407–1410
 35. Wen H, Shah J, Balaban RS (1998) Hall effect imaging. *IEEE Trans Biomed Eng* 45:119–124
 36. Ye SG, Harasiewicz KA, Pavlin CJ, Foster FS (1995) Ultrasound characterization of normal ocular tissue in the frequency range from 50 MHz to 100 MHz. *IEEE Trans Ultrason Ferroelectr Freq Control* 42(1):8–14
 37. Zeng X, Liu G, Xia H, Xu X (2010) An acoustic characteristics study of magneto-acousto-electrical tomography: a new method to reconstruct current density distribution at every point of a sample. 2010 3rd International Conference on Biomedical Engineering and Informatics. 16–18 Oct 2010. IEEE; Yantai, pp 95–98